RSC Advances

ROYAL SOCIETY OF CHEMISTRY

www.rsc.org/advances

Hydrothermally prepared chromia-alumina(xCr/Al_2O_3) catalysts with hierarchical structure for propane dehydrogenation

Wan-Zhong Lang*, Chang-Long Hu, Lian-Feng Chu, Ya-Jun Guo*

The Education Ministry Key Laboratory of Resource Chemistry and Shanghai Key Laboratory of Rare Earth Functional Materials, Department of Chemistry and Chemical Engineering, Shanghai Normal University, 100 Guilin Road, Shanghai 200234, P.R. China

* Corresponding author. Tel: +86-21-64321951; Fax: +86-21-64321951.

E-mail address: wzlang@shnu.edu.cn(W.Z. Lang), guoyajun@shnu.edu.cn(Y.J. Guo)

Abstract

Propane dehydrogenation was investigated over a series of chromia-alumina (xCr/Al_2O_3) catalysts containing 2.5-10wt.% chromium(Cr), synthesized via hydrothermal synthesis method. The synthesized xCr/Al_2O_3 catalysts with hierarchical spindle-like morphology have high specific area and highly dispersed chromia on the surface of γ-Al_2O_3. Besides, the higher Cr^{6+}/Cr^{3+} ratio is advantageous to obtain higher propane conversion and lower propylene selectivity. The synthesized 7.5Cr/Al_2O_3 catalyst exhibits the highest propane conversion of 62% accompanying with 89% propylene selectivity at 873K. After regenerated by re-calcinating in air, the original activity of spent catalyst is well recovered.

Key words: Propane dehydrogenation; Chromia-alumina catalysts; Hydrothermal systhesis; Hierarchical structure

1. Introduction

Propylene is an important basic chemical raw material, which can be used to produce polypropylene, epoxypropane, acrylonitrile, acrolein and other downstream products. Because of growing demand for propylene, much effort has been paid to new propylene production routes. Dehydrogenation of propane (DHP) or oxidative dehydrogenation of propane(ODHP) is a promising industrial alternative to produce propylene since it make low-value propane to high valuable propylene, which is now mainly produced by steam cracking and fluid catalytic cracking (FCC) process.

Supported chromia catalysts were intensively studied for the dehydrogenation of light alkanes. However, the deactivation of Cr-based catalysts due to the catalytic cracking and coking is a major challenge in DHP or ODHP process. [1,2,3,4] Therefore, it is important to develop supported chromia catalysts with high reactivity, selectivity and stability. To approach this aim, the various strategies, such as exploring preparation methods,[2,5,6,7,8,9] using novel carriers[10,11,12,13,14] and Cr precursors[15], introducing additives[16,17,18] etc. have been widely employed.

The chromia-alumina catalysts revealed in previous works are mainly prepared by the methods of co-precipitation, incipient wetness impregnation, atomic layer self-assembly, atomic layer deposition technique and so on.[1, 19,20,21,22] However, to our best knowledge, the utilization of hydrothermal method to synthesize CrO_x-Al_2O_3 catalysts for the dehydration of light alkanes has not been revealed. The hydrothermally prepared γ-Al_2O_3 with surfactant-assistance with hierarchical nanoarchitecture and high specific surface had been

revealed as effective adsorbents.[23] The hydrothermally prepared Cr_2O_3-ZrO_2 exhibited an enhanced catalytic reactivity compared to the conventional samples.[7] Pan also found that W/γ-Al_2O_3 catalysts prepared by a surfactant-assisted hydrothermal deposition method had higher dispersion of tungsten species, more open pore channels, and more acid sites, and thus presented a significantly enhanced hydrodenitrogenation activity compared with the catalyst prepared by impregnation.[24] In this work, the alumina-supported chromium oxides with hierarchical porous structure are synthesized and used as efficient catalysts in the dehydrogenation of propane. The catalysts exhibit high catalytic activity for the dehydrogenation of propane. The stuctrure-activitity relationship of the synthesized catalysts is analyzed upon numerous state-of-the-art analytical techniques.

2. Experimental

2.1 Preparation of catalysts

The catalysts were synthesized by direct hydrothermal method. The required amount of $Cr(NO_3)_3 \cdot 9H_2O$ and $Al(NO_3)_3 \cdot 9H_2O$ were dissolved in 80.0 g deionized water and stirred for 3 h at 333 K. Then 20.0 g tetrapropylammonium hydroxide(TPAOH) was added to the mixed solution and stirred overnight. The obtained solution was transferred to a teflon-linked stainless-steel autoclave and sealed. The autoclave was heated at 443 K for 3 days, and then cooled down to room temperature. After centrifuged, the obtained sample was dried at 373 K for 24 h, and then calcined at 823 K in air for 5 h. The catalysts were referred to as *x*Cr/Al_2O_3, where *x* represents the chromium loading (mass percent) on Al_2O_3.

2.2 Characterizations

XRD measurements were performed on a Bragg-Brentano diffractometer (Rigaku D /Max-2000) with monochromatic CuKa radiation (λ=1.5418 Å) of graphite curve monochromator in 10-80° with a scan speed of 4°/min. The ultraviolet-visible(UV-vis) spectra of the samples were performed on a spectrometer (UV-3600, Shimazdu) in the range of 230-1500 nm with $BaSO_4$ as reference. The morphologies of xCr/Al_2O_3 catalysts were examined by a field emission scanning electron microscopy (FESEM, HITACHI S-4800) and transmission electronic microscopy (TEM, JEM-2010). The N_2 adsorption-desorption isotherms were detected on a Quantachchrome NOVA 4000e. All samples were activated by degassing under vacuum at 573 K for 5 h before measuring. X-ray photoelectron spectroscopy (XPS) measurements were performed on a PHI5000 VersaProbeTM.

2.3 Propane dehydrogenation reaction

The catalytic propane dehydrogenation was performed at 873K in a fix-bed quartz reactor (8 mm in diameter) at atmosphere pressure. The feed flow was the mixed gas of propane and Argon ($V(C_3H_8)$：V(Ar) = 1:4) with a feed flow rate of 20 ml·min^{-1}. The catalyst (200 mg) was loaded into the reactor and pre-treated under Ar atmosphere for 30 min at 873K before propane dehydrogenation reaction. The products containing methane, ethylene, ethane, propylene and propane were analyzed with an on-line gas chromatograph(SP-6890, Shandong Lu'nan) with a micro FID detector.

2.4 TGA

The amount of carbon deposit on the spent sample was also determined by thermogravimetric analysis(TGA). TGA was measured in air flow (50 ml·min^{-1}) with a SHIMADZU DTG-60H thermogravimetric analyzer from room temperature to 1073K at the rate of 10 K/min.

3. Results and discussion

3.1 X-ray diffraction

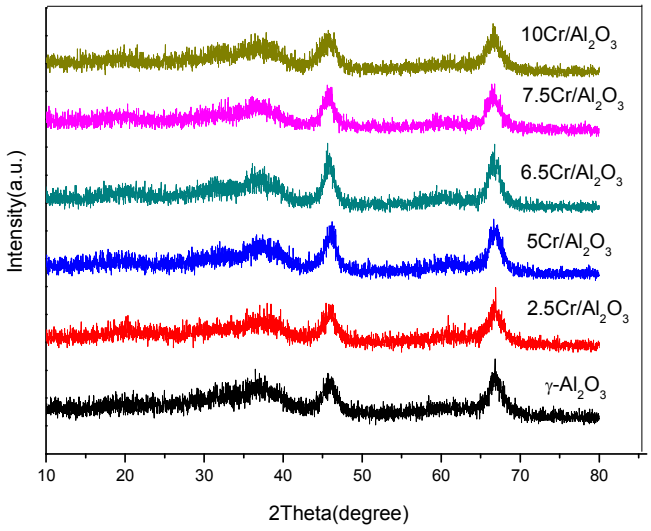

Fig.1. XRD patterns of *x*Cr/ Al_2O_3 catalysts.

The XRD patterns of *x*Cr/Al_2O_3 catalysts are shown in Fig.1. The peaks at 2θ=37.6°, 45.8° and 67.3° of all samples (including pure γ-Al_2O_3), which are attributed to the characteristic diffractions of γ-Al_2O_3,[23,24] are found in these samples. Furthermore, no diffraction peaks of chromia are observed due to its high dispersion state. The absence of CrO_x peaks could be attributed to small Cr particle size.

3.2 Morphologies of *x*Cr/Al_2O_3 catalysts and BET analysis

From Fig.2(a), the FESEM images show that the *x*Cr/Al_2O_3 catalysts exhibit hierarchical spindle-like morphology in this work. The similar nanohierarchical structure of γ-Al_2O_3 via surfactant-assisted hydrothermal method was also revealed.[23] With the addition of Cr, the particles grow and change to be more dispersive. The TEM images in Fig.2(b) show that these particles are comprised of a large number of nanoflakes with an average size of ca.1.8 μm in length and 400 nm in width. It was reported that the hydrogen bonds between the boehmite (precursor of γ-Al_2O_3) surface and template molecules can reduce the free energy of crystallites to form low dimensional nanoflakes.[33,34] These nanoflakes tend to aggregate and reduce exposed area in order to decrease the surface energy. Consequently, the hierarchical spindle-like particles are formed through the oriented self-assembly mediated by TPAOH.[33]

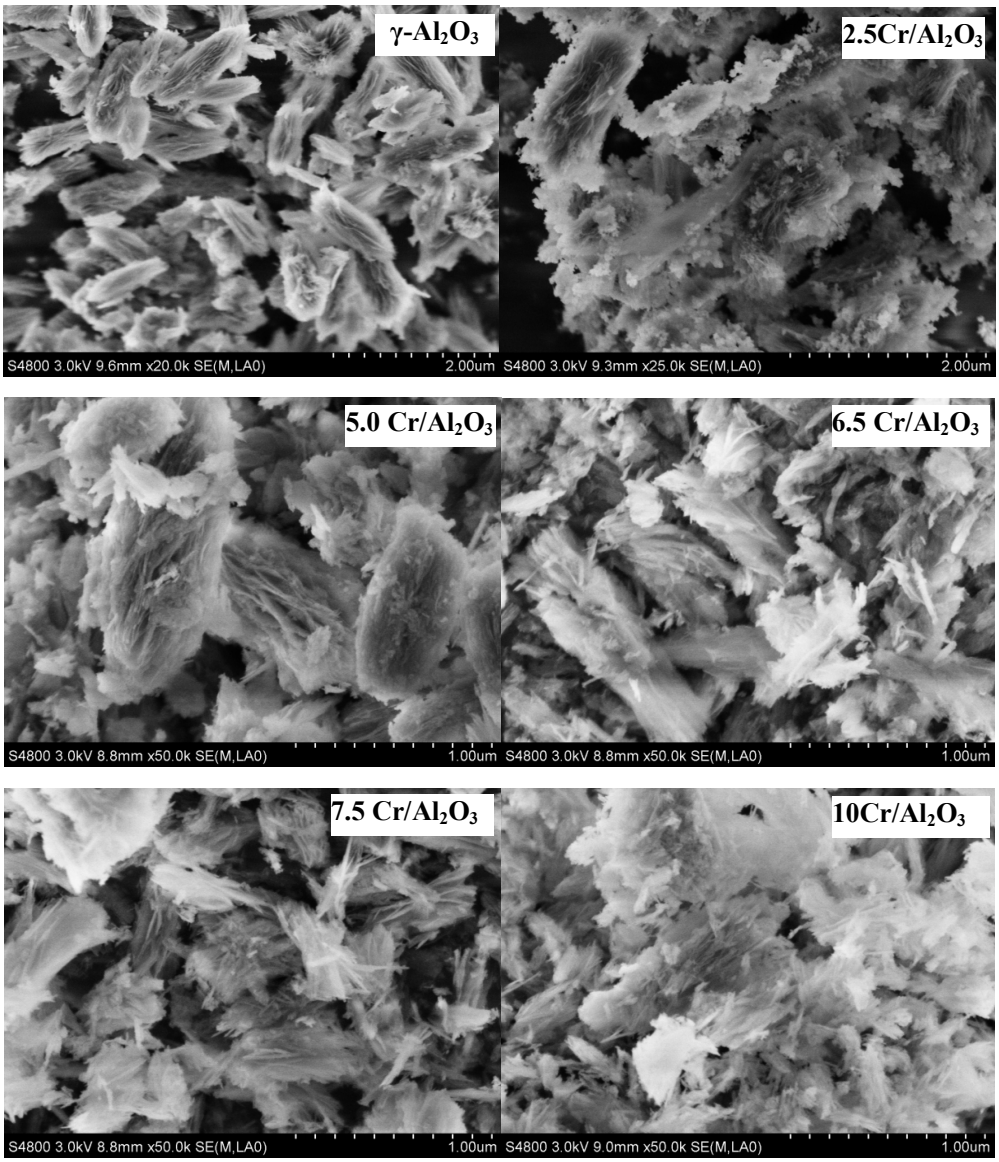

(a)

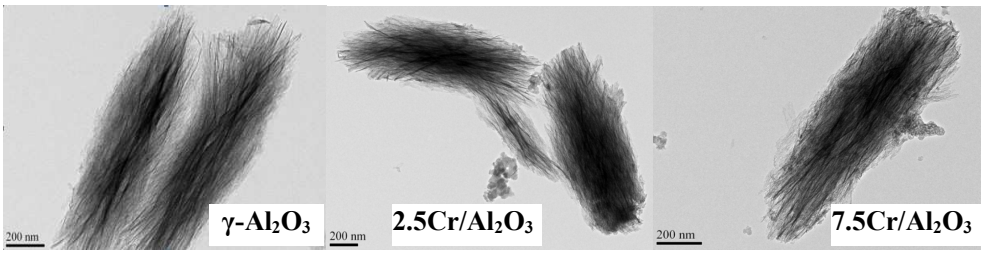

(b)

Fig.2 FESEM(a) and TEM(b) images of *x*Cr/ Al_2O_3 catalysts

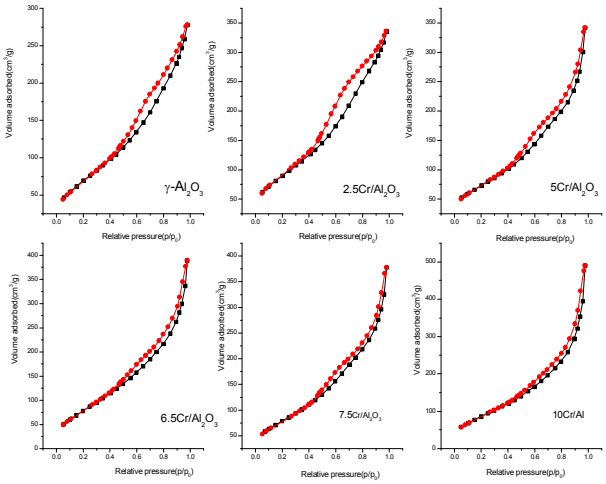

(a)

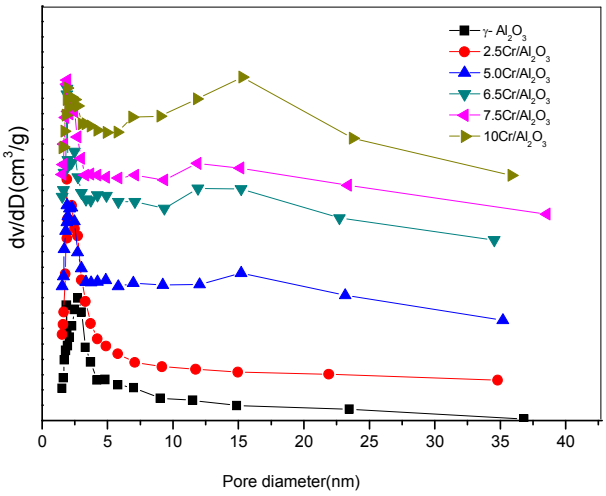

(b)

Fig.3 N_2 adsorption-desorption isotherms(a) and the pore size distributions (b) of *x*Cr/Al_2O_3 catalysts

The N_2 adsorption-desorption isotherms of xCr/Al_2O_3 catalysts are given in Fig.3(a). The samples display type IV adsorption isotherms with H_3-type weak hysteresis loops between 0.5 and 0.99, which is related to big slit-like mesopores. When P/P_0 is above 0.9, the isotherms rise sharply and do not appear S shape, indicating the samples contain macropores. These macropores may be produced by the tiny gaps between the neighboring nanoflakes of catalysts. Fig.3(b) shows that the samples present a comparatively sharper mesopore size distribution centered at 3.6-4.0 nm. When Cr loading exceeds 5.0 wt.%, the catalysts exhibit bimodal pore distribution with mesopores(ca. 3.8-4.0 nm) and macropores (ca.15 nm). The textural parameters of xCr/Al_2O_3 catalysts in table 1 show that all samples have high specific surface area(S_{BET}), moderate pore volume (V_P), and small average pore size (D_P). Additionally, the S_{BET}, V_P and D_P exhibit an increasing trend with the increase of Cr loading in the samples. It should be ascribed to the enhanced particle size and the dispersed nanoflakes, which is consistent with the morphologies shown in Fig.2.

Table 1 Textural properties of xCr/ Al_2O_3 catalysts

Samples	S_{BET} (m^2/g)	V_P (cm^3/g)	D_P (nm)
γ-Al_2O_3	250.232	0.428	3.742
2.5Cr/Al_2O_3	258.546	0.490	3.772
5.0Cr/Al_2O_3	261.391	0.505	3.828
6.5Cr/Al_2O_3	277.115	0.569	3.836
7.5Cr/Al_2O_3	282.334	0.621	3.840
10Cr/Al_2O_3	295.196	0.725	3.921

3.3 UV-vis spectra and XPS analysis of xCr/Al_2O_3 catalysts

To investigate the oxidation state of chromium, the diffuse reflectance UV-vis spectra of *x*Cr/Al_2O_3 catalysts were carried out and shown in Fig.4(a). All spectra show two intense absorption bands at 270 and 369 nm, which are attributed to O→Cr^{6+} charge transfer of chromate, verifying the presence of Cr^{6+} on the catalysts.[2, 20, 26, 35] The weak shoulders at 456 nm assigned to d-d transition (A_{2g}-T_{1g}) of Cr^{3+} in octahedral symmetry.[3, 15] Another weak band at ~600 nm should be ascribed to another d-d transition (A_{2g}-T_{2g}) of Cr^{3+} in octahedral symmetry.[3, 15]

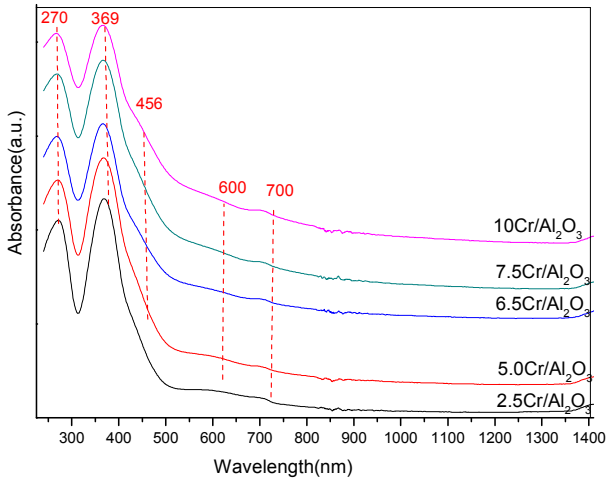

(a)

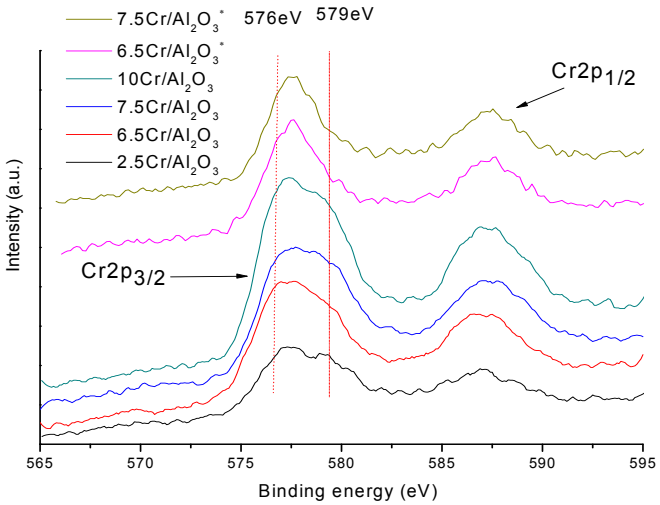

(b)

Fig. 4 Diffuse reflectance UV-vis spectra(a) and XPS spectra(b) of *x*Cr/Al_2O_3catalysts

Table 2 XPS data of *x*Cr/Al_2O_3 catalysts(*-the spent catalysts)

Catalysts	Cr $2p_{3/2}$ B.E.(eV)		Cr^{6+}%	Cr^{6+}/Cr^{3+}	$(Cr/Al)_{xps}$
	Cr^{6+}	Cr^{3+}			
2.5Cr/Al_2O_3	579.550	576.841	0.779	0.428	0.0426
6.5Cr/Al_2O_3	579.173	576.651	3.22	1.080	0.0777
7.5Cr/Al_2O_3	579.141	576.814	4.52	1.314	0.0971
10Cr/Al_2O_3	579.127	576.864	4.94	1.034	0.1220
6.5Cr/Al_2O_3*	579.771	576.455	0.402	0.096	/
7.5Cr/Al_2O_3*	579.589	576.399	0.757	0.176	/

The XPS spectra of *x*Cr/Al_2O_3 catalysts are shown in Fig.4(b). The binding energy values corresponding to $Cr2p_{3/2}$ are shown in table 2. The oxidation states of Cr^{6+} and Cr^{3+} are found for all catalysts at ~579 eV and ~576 eV.[27,28,29,30] The XPS results also verify the existence of Cr^{6+} and Cr^{3+}, which agrees with the UV-vis spectra of *x*Cr/Al_2O_3 catalysts. The Cr^{6+}% and

Cr^{6+}/Cr^{3+} ratios are calculated from the deconvoluted Gaussian fitting from the $Cr2p_{3/2}$ peaks shown in Fig.5. It can be seen that the Cr^{6+}/Cr^{3+} ratio varies with Cr loading, which influences the catalytic activity of Cr-based catalysts.[15, 35] In addition, XPS is an effective method to study the dispersion of transition metal oxides on supports. Many researchers adopt the surface atomic ratios of the active metal elements to the element of the support as a measure of the dispersion of the catalysts.[31,32] The atomic ratio of $x Cr/Al_2O_3$ catalysts detected by XPS ($(Cr/Al)_{XPS}$) in table 2 increases almost linearly as Cr loading increases. This indicates that the chromium species is well dispersed over the investigated range of Cr loading, which is consistent with the XRD results.

3.4 Catalytic performances of $x Cr/Al_2O_3$ catalysts on propane dehydrogenation reaction

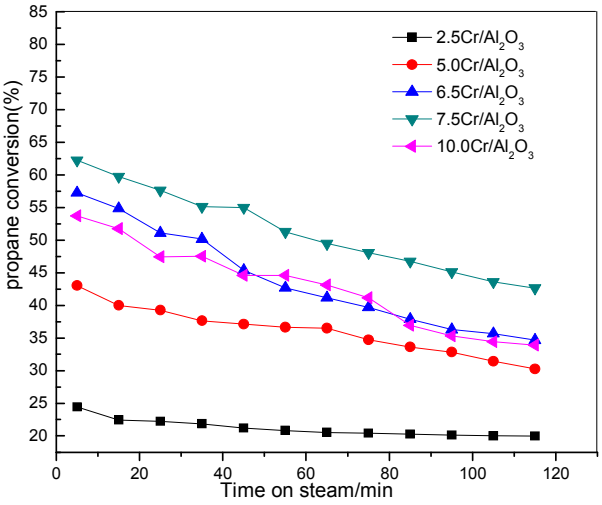

(a)

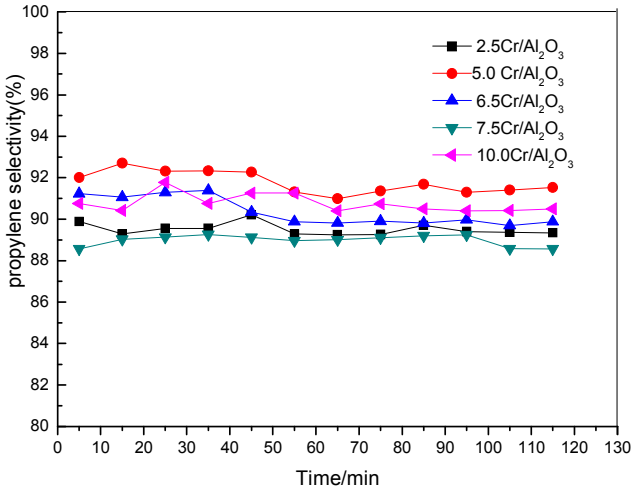

(b)

Fig.5 Propane conversion(a) and propylene selectivity(b) over *x*Cr/Al_2O_3 catalysts versus time on stream (Reaction conditions: $V_{(C3H8)}$:$V_{(Ar)}$=1:4, total flow rate =20 ml·min^{-1}, T=873K).

The propane conversion and propylene selectivity versus time on steam over the *x*Cr/Al_2O_3 catalysts are shown in Fig.5. It is observed from Fig.5(a) that the propane conversion increases with increasing Cr loading from 2.5wt.% to 7.5wt.%, and then decreases by further adding Cr to 10.0wt.%. However, the improved propane conversion with increasing Cr loading may be obtained at the cost of propylene selectivity. From Fig.5(b), the lowest propylene selectivity is obtained over 7.5Cr/Al_2O_3, which has the highest initial propane conversion of 62.2%. It also can be seen that the propane conversion for all samples decreases with time on steam due to the coke and deactivation of catalysts during the reaction process; while the selectivity varies little. The literatures revealed that the oxidative states of chromium species were key to the catalytic dehydrogenation activity of light alkanes though it is still controversial up to now. [1, 35,36] As discussed earlier in this work, the UV-vis and XPS

data of xCr/Al_2O_3 catalysts demonstrate the existence of Cr^{6+} and Cr^{3+} species. The surface Cr^{6+}/Cr^{3+} ratios of xCr/Al_2O_3 catalysts are different, which influences the reducibility of catalysts. By comprehensively analyzing the catalytic activity and XPS data, the higher Cr^{6+}/Cr^{3+} leads to a higher propane conversion and a lower Cr^{6+}/Cr^{3+} propylene selectivity. The Cr^{6+}% and Cr^{6+}/Cr^{3+} of the spent catalysts of 6.5Cr/Al_2O_3 and 7.5Cr/Al_2O_3 are much lower than those of the corresponding fresh catalysts (table 2). Hence, Cr^{6+} species is reduced to Cr^{3+} in DHP process. This suggests that Cr^{6+} species are important for DHP reaction. The similar catalytic dehydrogenation of isobutene over other Cr_2O_3-Al_2O_3 catalysts were reported by Xu *et al*.[35]

The time-on-stream study of 7.5Cr/Al_2O_3 catalyst is carried out for about 10 hours and is presented in Fig.6. It can be seen that the propane conversion decreases above 62.0% to 25.7% after about 10 hours, but the propylene selectivity has nearly no change.

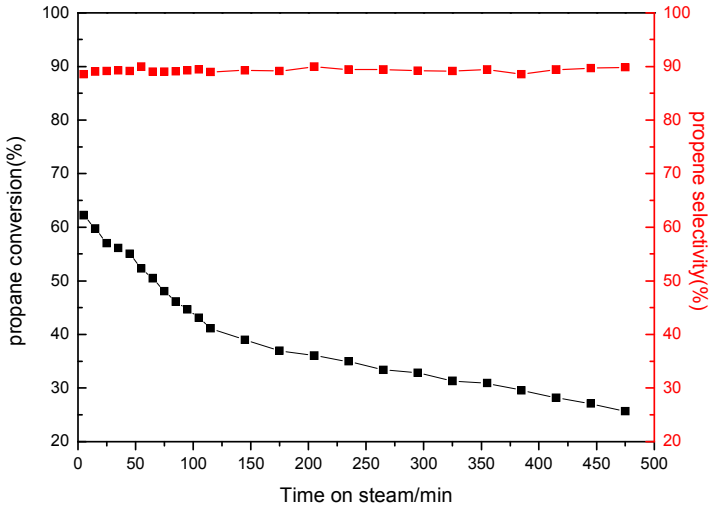

Fig. 6 Stability test of 7.5Cr/Al_2O_3 catalyst in propane dehydrogenation (Reaction conditions: $V_{(C3H8)}$:$V_{(Ar)}$=1:4, total flow rate =20 ml·min^{-1}, T=873K).

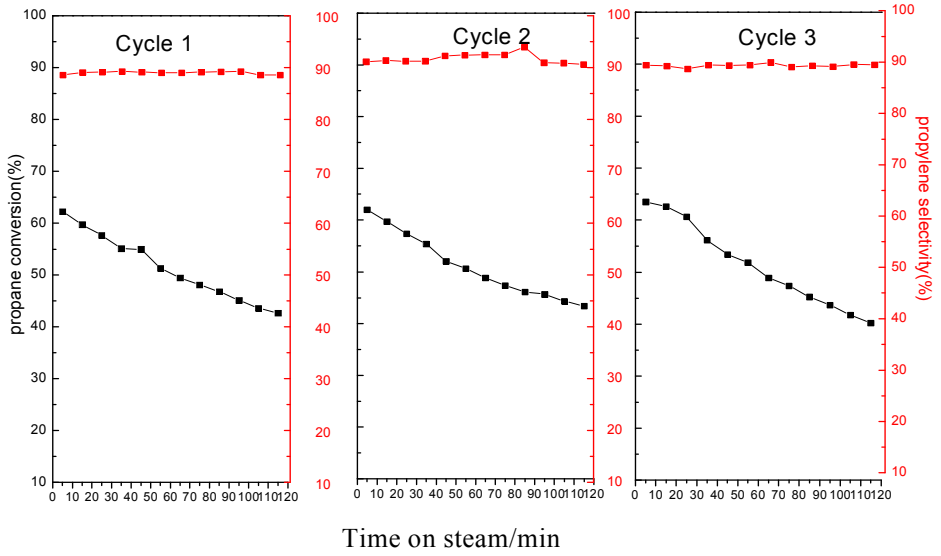

Fig.7 Reuse of 7.5Cr/Al_2O_3catalyst (Reaction conditions: $V_{(C3H8)}$:$V_{(Ar)}$=1:4, total flow rate =20 ml·min^{-1}, T=873K)

The spent 7.5Cr/Al_2O_3 catalyst is regenerated by re-calcinating in air for 5 h. The recycle of 7.5Cr/Al_2O_3 catalyst for propane dehydrogenation reaction is presented in Fig.7. It can be seen that the initial propane conversions in three recycles are all above 60.0 %, and the propylene selectivity varies little, indicating that the original activity of the catalyst is well recovered. Little difference in the activity is observed before and after regeneration.

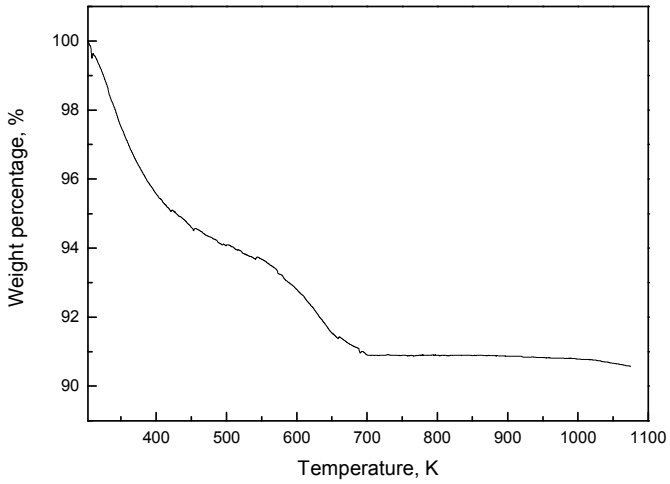

Fig.8 Thermogravimetric analysis (TGA) of spent 7.5Cr/Al_2O_3 catalyst

Thermogravimetric analysis of spent 7.5Cr/Al_2O_3 catalyst is performed in air atmosphere and illustrated in Fig.8. It can be seen that weight loss can be divided into two stages: room temperature to 473 K and after 473 K. The former stage is mainly attributed to the loss of adsorbed water and organic species. The second stage can be attributed to the burning of coke. According to the result in Fig.8, the deposited coke is about 3.67wt.% for the spent 7.5Cr/Al_2O_3 catalyst.

4. Conclusion

In the present study, the CrO_x-Al_2O_3 catalysts with hierarchical architecture were hydrothermally synthesized and applied to DHP process. The prepared CrO_x-Al_2O_3 catalysts were well characterized by numerous state-of-the-art analytical techniques. The XPS and diffuse reflectance UV-vis spectra confirm that the existence of Cr^{6+} and Cr^{3+}, and the Cr^{6+}/Cr^{3+} ratio varies with the Cr loadings of *x*Cr/Al_2O_3 catalysts. The propane conversion increase firstly with Cr loading and attain a peak point with 7.5% Cr loading, and then

decreases with the further Cr loading in the catalysts. This variation trend is identical to the Cr^{6+}/Cr^{3+} ratio in xCr/Al_2O_3 catalysts, implying that Cr^{6+} species are important for DHP reaction. The synthesized 7.5Cr/Al_2O_3 catalyst exhibits the highest propane conversion of 62% accompanying with 89% propylene selectivity at 873K. After regenerated by re-calcinating in air, the original activity of spent catalyst is well recovered.

Acknowledgments

The research is supported by Shanghai Municipal Natural Science Foundation (13ZR1429900), Innovation Program of Shanghai Municipal Education Commission (), Program for Changjiang Scholars and Innovative Research Team in University (IRT1269) and Internation Joint Laboratory on Resource Chemistry (IJLRC).

References

1 M. Santhosh Kumar, N. Hammer, M. Rønning, A. Holmen, D. Chen and G. Øye, *J. Catal*., 2009, **261**, 116-128.

2 P. Michorczyk, P. Pietrzyk and J. Ogonowsk, *Microporous Mesoporous Mater*., 2012, **161**, 56–66.

3 D. Shee, A. Sayari, *Appl Catal A: Gen*., 2010, **389**,155–164.

4 M. A. Botavina, G. Martra, Yu. A. Agafonov, N. A. Gaidai, N. V. Nekrasov, D. V. Trushin, S. Coluccia and A. L. Lapidus , *Appl. Catal., A: Gen*., 2008, **347**, 126–132.

5 I. Martyanov, A. Sayari, *Catal Lett*., 2008, **126**,164–172.

6 M. A. Botavina, C. Evangelisti, Yu, A. Agafonov, N. A. Gaidai, N. Panziera, A. L. Lapidus and G. Martra, *Chem. Eng. J.*, 2011, **166**, 1132–1138.

7 R .X. Wu, P .F. Xie, Y. H. Cheng, Y. H. Yue, S. Y. Gu, S. Y. Gu, W. M. Yang, C. X. Miao , W. M. Hua and Z. Gao, *Catal. Commun*., 2013, **39**, 20-23.

8 J. Janas, J. Gurgul, R. P. Socha and J. Kowalska, *J. Phys. Chem. C*.,2009, **113**, 13273–13281.

9 A. Verma, R. Dwivedi, P. Sharma and R. Prasad. *RSC Adv*., 2014, **4**, 1799-1807.

10 F. Zhang, R. X. Wu, Y. H. Yue, W. M. Yang, S. Y. Gu, C. X. Miao, W. M. Hua and Z. Gao, *Microporous and Mesoporous Mater*., 2011, **145** , 194–199.

11 P. Michorczyk, K. Gora-Marek and J. Ogonowski, *Catal. Lett*., 2006, **109**, 195-198.

12 J. Baek, H. J. Yun, D. Yun, Y. Choi and J. Yi, *ACS Catal*., 2012, **2**, 1893−1903.

13 Q. Zhu, M. Takiguchi, T. Setoyama, T. Yokoi, J.N. Kondo and T. Tatsumi, *Catal Lett*., 2011, **141**, 670–677.

14 C. Boucetta, M. Kacimi, A. Ensuque, J.Y. Piquemal, F.B. Verduraz and M. Ziyad, *Appl Catal A: Gen*.,2009, **356**, 201–210.

15 H. Zhao, H. Song, L. Xu and L. Chou, *Appl Catal A: Gen*., 2013, **456**, 188–196.

16 E. Rombi, D. Gazzoli, M.G. Cutrufello, S. De Rossi and I. Ferino, *Appl Surf Sci*., 2010, **256**, 5576–5580.

17 J. Słoczyński, B. Grzybowska, A. Kozłowska, K. Samsona, R. Grabowski, A. Kotarba and M. Hermanowska, *Catal Today*., 2011, **169**, 29–35.

18 M. Cherian, R. Gupta, M.S. Rao and G. Deo, *Catal Lett*. ,2003, **86**,179-189.

19 L. R. Mentasty, O. F. Gorriz and L. E . Cadus , *Ind. Eng. Chem. Res*.,1999, **38**, 396-404.

20 F. Cavani, M. Koutyrev, F. Trifirò, A. Bartolini, D. Ghisletti, R. Iezzi, A. Santucci and G. Del Piero, *J. Catal*., 1996, **158**, 236–250.

21 A. Hakuli, A. Kytökivi and A. O. I . Krause, *Appl Catal A: Gen*., 2000, **190**,219–232.

22 S. M. K. Airaksinen, A. O. I. Krause, *Ind. Eng. Chem. Res*., 2005, **44**,3862-3868.

23 W. Wang, J. Zhou, Z. Zhang, J. Yu and W. Cai, *Chem. Eng. J*., 2013, **233** , 168–175.

24 Y. Fan, X. J. Bao, H. Wang, C. F. Chen and G. Shi , *J. Catal*.,2007, **245**, 477–481.

25 Y. C. Xie, Y.Q. Tang , *Adv. Catal*., 1990, **37**,1-43.

26 P. Michorczyk, J. Ogonowski, P. Kuśtrowski, *Appl. Catal., A: Gen*., 2008, **349**,62-69.

27 X. J. Shi, S. Ji, K. Wang and C. Y. Li, *Energy Fuels*., 2008, **22**,3631-3638.

28 S. Kilicarslan, M. Dogan and T. Dogu, *Ind. Eng. Chem. Res*., 2013, **52**, 3674-3682.

29 D. L. Hoang, A. Dittmar, J. RAdnil, K.W. Brzezinka and K. Witke, *Appl. Catal*., A., 2003, **239**, 95- 110.

30 S. Deng, S. Li, H. Li and Y. Zhang, *Ind. Eng. Chem. Res*., 2009, **48**,7561-7566.

31 H. Wang, Y. Fan, G. Shi , Z. H. Liu , H. Y. Liu and X. J. Bao, *Catal. Today*., 2007, **125**, 149-154.

32 B. M. Reddy, B .Chowdhury, E .P. Reddy and A. Fernández, *Appl. Catal*., A., 2001, **213**, 279-288.

33 J. Ge, K.J. Deng, W. Q. Cai,X.Q.Yu, X. Q. Liu and J. B. Zhou, *J. Colloid Interface Sci*., 2013, **401**, 34-39.

34 L. Pan, Z. Sun and C. Q. Sun, *Mater. Chem. A*.,2013, **1**, 8299-8326.

35 L. Xu, Z. L. Wang, H. L. Song and L. J. Chou, *Catalysis Commu.*, 2013, 35,76-81.

36 B.Y. Jibril, N. O. Elbashir and S. M. Al-Zahrani, *Chem. Eng. Process.*, 2005, **44**,835-840.

Figure captions

Fig.1 XRD patterns of *x*Cr/Al_2O_3 catalysts

Fig.2 FESEM(a) and TEM(b) images of *x*Cr/Al_2O_3 catalysts

Fig.3 N_2 adsorption-desorption isotherms(a) and pore size distributions (b) of *x*Cr/Al_2O_3 catalysts

Fig. 4 Diffuse reflectance UV-vis spectra(a) and XPS spectra(b) of *x*Cr/Al_2O_3 catalysts

Fig.5 Propane conversion(a) and propylene selectivity(b) over *x*Cr/Al_2O_3 catalysts versus time on stream (reaction condition: catalyst mass: 200mg; feed gas: $V_{(C3H8)}$:$V_{(Ar)}$=1:4; total feed flow : 20 ml·min^{-1}; temperature: 873K).

Fig. 6 Stability test of 7.5Cr/Al_2O_3 catalyst in propane dehydrogenation (Reaction conditions: $V_{(C3H8)}$:$V_{(Ar)}$=1:4, total flow rate =20 ml·min^{-1}, T=873K).

Fig.7 Reuse of 7.5Cr/Al_2O_3catalyst (Reaction conditions: $V_{(C3H8)}$:$V_{(Ar)}$=1:4, total flow rate =20 ml·min^{-1}, T=873K)

Fig.8 Thermogravimetric analysis (TGA) of spent 7.5Cr/Al_2O_3 catalyst

Table captions

Table 1 Textural properties of xCr/Al_2O_3 catalysts

Table 2 XPS data of xCr/Al_2O_3 catalysts